Hindawi
Geofluids
Volume 2021, Article ID 7496540, 16 pages
https://doi.org/10.1155/2021/7496540

Research Article

Analysis on the Shape and Impact Pressure of the High-Pressure Water Jet during the Hydraulic Flushing Cavity Technique

Shouqing Lu,[1,2] Chengfeng Wang,[1,2] Wei Wang,[3] Mingjie Li,[1,2] and Dongti Zhang[4]

[1]*Department of Safety Engineering, Qingdao University of Technology, Qingdao 266520, China*
[2]*Shandong Key Industry Field Accident Prevention Technology Research Center (Non-Ferrous Metallurgy), Qingdao 266520, China*
[3]*Shanghai Fire Research Institute of MEM, Shanghai 200032, China*
[4]*School of Civil and Resource Engineering, University of Science and Technology Beijing, Beijing 100083, China*

Correspondence should be addressed to Wei Wang; wangweiwangwei0037@163.com

Received 13 April 2021; Accepted 22 May 2021; Published 18 June 2021

Academic Editor: Feng Du

A large proportion of minable coal seams in China belong to low-permeability soft coal seams. Such coal seams suffer serious coal and gas outburst hazards and endure a high incidence of major disasters in coal mines. The adoption of the high-pressure water jet (HPWJ) hydraulic flushing cavity can effectively promote the gas drainage efficiency and volume and eliminate the hidden danger of gas disasters. Nevertheless, the shape and impact pressure of rotating HPWJ are rarely researched. In this study, on the basis of the numerical simulation, the axial and radial stress distributions of HPWJ and the energy-gathering effect of a conical-cylindrical combined nozzle were analyzed. It is concluded that the submerged condition will accelerate the attenuation of jet velocity and reduce the impact strength of the jet. The jet diffusion angle grows with the increases in the nozzle diameter and water pressure, and 24° is the optimal contraction angle. Finally, the influences of factors such as the rotation speed on the shape and impact pressure of HPWJ were explored, and the results show that the rotation speed should be controlled within 90 r/min. The research findings lay the foundation of the study on the mechanism of coal crushing by HPWJ and provide technical support for the research and development of drilling and flushing integrated equipment.

1. Introduction

China, a country where over 95% of coal mines are recovered by means of underground mining [1–4], is suffering the most serious coal and gas outburst disasters in the world [5–7]. It contains a large number of outburst coal mines where outburst disasters occur intensely and frequently [8]. Low-permeability coal seams where gas can hardly be drained refer to the coal seams whose permeability λ is smaller than $0.1\ m^2/(MPa^2{\cdot}d)$ [9], and soft coal seams refer to the coal seams whose hardness coefficient f is smaller than 1 [10]. Low-permeability soft coal seams account for a large proportion of mineable coal seams in China. For a long time, it is difficult to control gas in high-gas soft coal seams due to low permeability and poor drilling stability [11, 12], and the fatality rate of gas accidents in coal mines remains high [13–15]. Therefore, high-gas soft coal seams endure a high incidence of major disasters in coal mines [16, 17]. The hydraulic flushing cavity technique works by drilling along-measure boreholes or cross-measure boreholes into the coal body and then flushing out large quantities of coal and gas through the high-pressure water jet (HPWJ) [18, 19]. The multiple large-diameter cavities formed in the coal seam are conducive to pressure relief and gas release. This technique, together with gas drainage measures, serves to reduce the ground stress and gas pressure of coal. It can effectively promote the gas drainage efficiency and volume and eliminate the hidden danger of mine gas disasters, thus providing a new approach for gas control in high-gas soft coal seams.

HPWJ, a coal/rock crushing technique, is widely applied to coal and petroleum fields in recent years [20]. The technique boasts multiple advantages such as concentrated energy transfer, no spark, no wear, no generation of high temperature or static electricity, dust reduction, and strong adaptability. Thanks to these advantages, it is particularly competent to crush coal and release gas in high-gas low-

permeability coal seams [21, 22]. Scholars all over the world have conducted extensive research studies on rock crushing by HPWJ and have proposed a variety of theories, including the water hammer effect theory, the stress wave effect theory, the impact effect theory, the water wedge effect theory, the cavitation effect theory, and the pulsed load-induced fatigue damage theory [23–26] The stress wave effect theory proposed by Singh and Hartman [27] in 1961 is the earliest accessible theory about rock crushing and failure under the action of jets. Based on this theory, Farmer and Attewell [28] put forward an empirical formula for the jet cutting depth and the P-wave velocity, i.e., the sound velocity.

Pan and Yao [29] and Bai and Cao [30] established a simulation model of rock crushing by pulsed water jets based on the arbitrary Lagrangian-Eulerian (ALE) algorithm, simulated the process of rock crushing with different-velocity jets, and studied the process of rock crushing damage evolution. Ma et al. [31] and Wang et al. [32] established a model of material cutting by HPWJ and a model of material erosion by abrasive jets by means of finite element modeling (FEM) and smoothed particle hydrodynamics (SPH). Based on the simulation data, they obtained the variation curves of the maximum cutting depth with the HPWJ velocity and the abrasive jet velocity, respectively, and verified the feasibility of the model by comparing the simulation data with the experimental results. Maniadaki et al. [33] and Gong et al. [34] established a numerical model of material erosion by HPWJ and a model of material cutting by premixed abrasive water jets based on the ALE algorithm.

Ni et al. [35–38] researched the process and mechanism of HPWJ flushing. By regarding the damage variable as the criterion of rock failure, they established a coupling model of HPWJ-induced macro/micro rock damage. Wang et al. [39, 40] simulated the process of HPWJ-induced rock crushing by means of nonlinear dynamic FEM and rock dynamic damage modeling. They drew the following conclusions. (1) HPWJ can crush the rock in milliseconds. (2) The rock crushing mechanism of ordinary continuous HPWJ is to cause tensile failure as a result of pressure relief and jet impact. (3) The process of rock crushing proceeds stepwise. Song and Chen [41] simulated the process of HPWJ-induced rock crushing based on the SPH algorithm and analyzed the energy conversion in this process, the impact force of HPWJ, and the evolution of HPWJ-induced rock crushing. Lu et al. [42] simulated the stress wave effect of the pulsed water jet in the process of rock crushing by using the SPH algorithm, concluding the failure modes of rocks with different lithologies under the pulsed water jet stress wave. By employing the ALE algorithm, Liu and Si [43] revealed that the confining pressure caused by HPWJ impact had a significant effect on the axial damage of rock and a slight effect on the radial damage. Lu et al. [24] conducted a test study on the mechanism of rock crushing by cavitating HPWJ, and Tian and Lin [25, 26] probed into the mechanism of jet-assisted rock crushing from two aspects, i.e., bubble cavitation and water drop impact. Si et al. [44] established a model of rock crushing by abrasive water jets from two perspectives, i.e., continuous damage mechanics and meso-damage mechanics.

Li [45] consolidated coal blocks with cement and obtained the variation of erosion depth with the pump pressure and target distance. Jiang [46] prepared coal rock specimens by mixing coal, sand, and cement at a certain ratio and performed experiments with an impeller rotary nozzle. Through these experiments, he found variations of erosion depth and width with the spray distance and nozzle diameter. Zhang [47] simulated the process of coal rock (replaced with concrete in his simulation) cutting by HPWJ and discussed the relationship among jet pressure, discharge quantity, and cutting volume and depth. Wang et al. [48] adopted an abrasive jet cutting system to cut argillaceous limestone in a coal seam floor and elaborated on the relationship between the cutting depth and the factors including the target distance, nozzle movement velocity, and number of reciprocation times. Sun et al. [49] simulated HPWJ-induced rock crushing in light of the dynamic nonlinear FEM and the Hoffman crushing criterion. They disclosed that the rock crushing efficiency could be promoted by increasing the impact velocity, jet diameter, transverse movement velocity, and jet beam number and reasonably selecting a jet incident angle in the range of 35~40°. Lin et al. [50] simulated the process of rock crushing by abrasive water jets through SPH-FEM. On the basis of the simulation results, they analyzed the range of rock damage by different-velocity abrasive water jets under the abrasive concentration of 30%.

The HPWJ, of which the medium is water, refers to a jet stream with a high impact velocity and a high dynamic pressure produced via a pressurizing device (pump station) and a nozzle of a specific shape. Its shape and impact pressure are mainly affected by conditions such as the pump pressure, pipeline resistance, nozzle structure, nozzle rotation speed, and environmental medium. In this study, numerical simulation was carried out with the assistance of ANSYS Fluent software. On the basis of the simulation, the axial and radial stress distributions of HPWJ and the energy-gathering effect of a conical-cylindrical combined nozzle were analyzed. Furthermore, the influences of the submergence conditions, nozzle diameter and angle, pump station pressure, rotation speed on the shape, and impact pressure of HPWJ were explored. The research findings facilitate the study on the mechanism of HPWJ-induced coal crushing and provide technical support for the research and development of drilling and flushing integrated equipment.

2. Impact Characteristics and Shape of HPWJ

2.1. Impact Characteristics of HPWJ. According to its different mechanisms, the HPWJ impact pressure on rock can be divided into two stages, namely, the water hammer pressure stage and the stagnation pressure stage. Sevda [51] generated an impact jet by dropping a hammer from a height to impact the piston. In this way, he successfully monitored the variations of impact pressure on different solid materials (Figure 1). The value of the rising angle θ is related to the transient reaction rate of the impacted material, and the reaction rate of metal materials is higher than that of polymer materials.

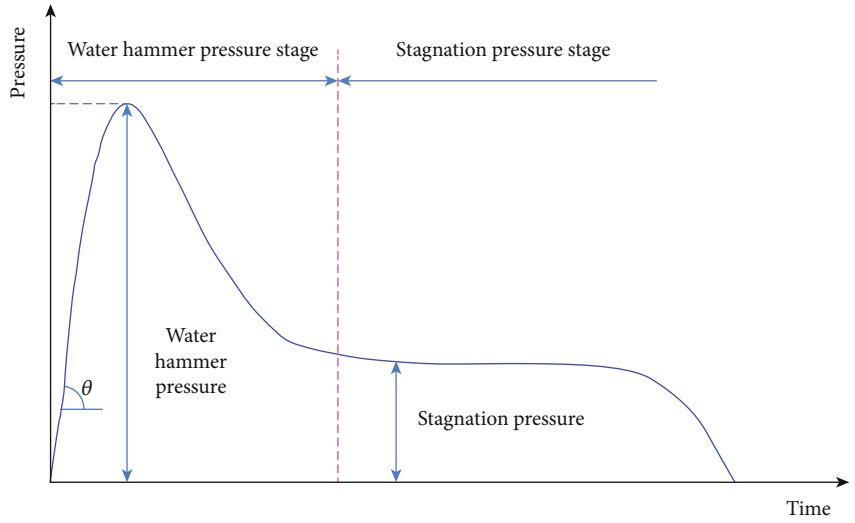

Figure 1: Division of the HPWJ impact pressure stage.

The inertia and compressibility of water are the main reasons for the generation of water hammer pressure. The shape of HPWJ is simplified as a cylinder (Figure 2). In the initial stage, the jet compression zone will be formed under the high-speed collision between the jet and the target. And the peak pressure with strong erosion force will be formed on the target surface when the water is compressed, that is, the water hammer pressure [52]. According to the law of conservation of momentum [53], the water hammer pressure can be derived as follows:

$$P_{\mathrm{wh}} = \frac{v\rho_{\mathrm{w}}c_{\mathrm{w}}\rho_{\mathrm{s}}c_{\mathrm{s}}}{\rho_{\mathrm{w}}c_{\mathrm{w}} + \rho_{\mathrm{s}}c_{\mathrm{s}}}, \tag{1}$$

where P_{wh} is the water hammer pressure, Pa; v is the velocity of water jet impact, m/s; ρ_{w} and c_{w} are the density of water and the velocity of shock wave propagation in the water medium, respectively, kg/m^3 and m/s; ρ_{s} and c_{s} are the density of rock and the velocity of shock wave propagation in rock, respectively, kg/m^3 and m/s.

The duration of water hammer pressure, which is generally in nanoseconds (ns), can be expressed as

$$t_r = \frac{r}{c_{\mathrm{w}}}, \tag{2}$$

where r is the radius of the jet, m; t_r is the duration of water hammer pressure, s.

After the water jet gets stabilized, it gradually enters the stagnation pressure stage where the Bernoulli stagnation pressure P_{s} is

$$P_{\mathrm{s}} = \frac{\rho_{\mathrm{w}}v^2}{2}, \tag{3}$$

where P_{s} is the Bernoulli stagnation pressure, Pa.

2.2. Influence of Submerged/Nonsubmerged Conditions on the Impact Characteristics and Shape of HSWJ. At present, scholars all over the world mostly adopt a high-speed camera for recording the shape of HPWJ [55–57] and analyzing its radial and axial structural characteristics. After the HPWJ is ejected from the nozzle, its front end gradually diffuses in the shape of an arc. Afterwards, the jet profile continues to expand and the diameter gradually increases until the water flow is completely dispersed. As exhibited in Figure 3, the HPWJ is of varying shapes in four primary sections, i.e., the compact section, the core section, the fracture section, and the dissipation section [58].

According to media in the surrounding environment, water jets can be divided into submerged water jets and nonsubmerged water jets. The analysis on a nonsubmerged water jet is chiefly focused on its diffusion law and core section length [59]. The core section where a great deal of energy is accumulated plays a decisive role in jet impact performance, while the outer boundary generally expands linearly in accordance with the angle. From statistics obtained by different research methods, Huang [60] found that the core section length of the jet is generally 400%~922% of the nozzle diameter and the jet diffusion angle generally ranges from 26.6° to 29.9°. Within the basic section, jet diffusion is rarely affected by the boundary layer and the nozzle, and it follows Equation (4) [61]:

$$d = k\sqrt{x}, \tag{4}$$

or

$$\frac{d}{R_0} = k_1\sqrt{\frac{x}{R_0}}, \tag{5}$$

where d is the jet diameter, m; x is the distance from the nozzle outlet, m; R_0 is the radius of the nozzle outlet, m; k and k_1 are the coefficients related to the nozzle,0020where $k_1 = 0.12 \sim 0.18$.

To explore the influence of the submerged condition on the impact characteristics and shape of HPWJ, the numerical

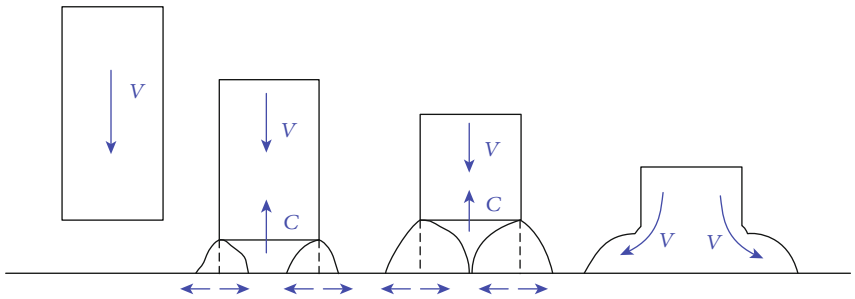

Figure 2: Schematic diagram of the initial stage of water jet impact on the solid surface [54].

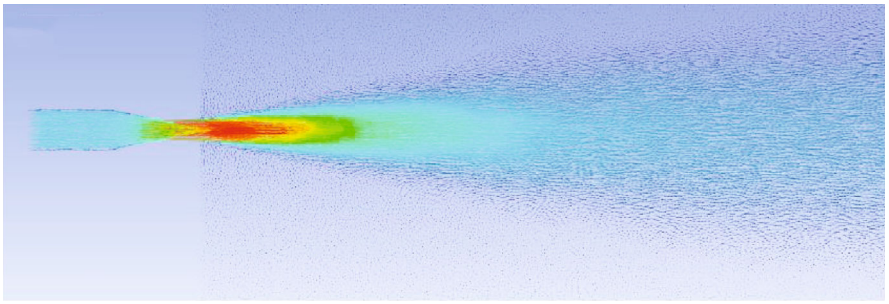

(a)

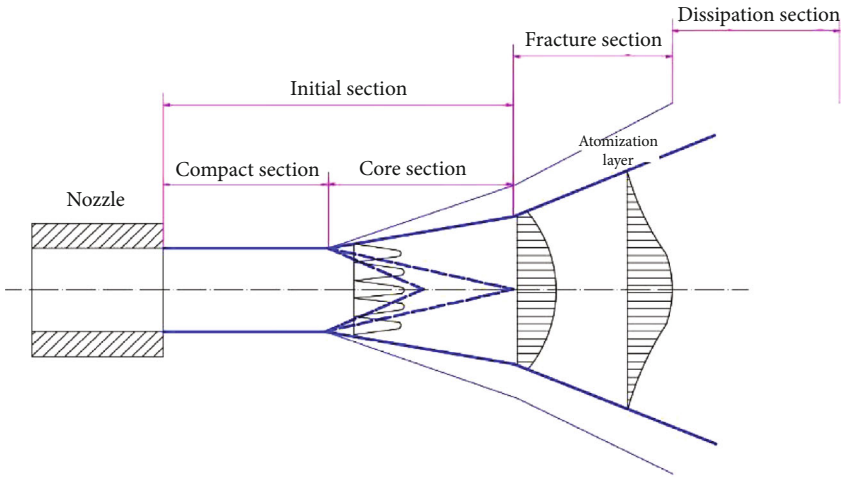

(b)

Figure 3: Shape of the water jet.

models of nonsubmerged and submerged jets were constructed, respectively, as shown in Figure 4(a). In the models, the jet impact distance (i.e., the target distance) was set to 100 mm, and the diameter of the circular rigid plate is 60 mm. Next, the jets under the submerged and nonsubmerged conditions were numerically calculated, respectively, with the calculation results displayed in Figures 4(b) and 4(c).

Under the nonsubmerged condition, the jet corresponds to slower velocity attenuation, a smaller diffusion angle, a larger initial section length, and a longer effective impact distance. The jet impact force on the axis of the rigid plate with the target distance of 100 mm can reach 80.7 MPa under the nonsubmerged condition, while it decreases to 65.2 MPa by 19.2% under the submerged condition. This demonstrates that the submerged condition will weaken the jet impact strength, thus affecting the coal crushing effect and the flushing efficiency. Therefore, in underground coal mines, HPWJ flushing operations should be carried out under the nonsubmerged condition. To achieve this goal, it is necessary to keep the drainage channel unobstructed.

2.3. Axial Dynamic Pressure Distribution of HPWJ. Dynamic pressure, which can be expressed by Equation (6), refers to the kinetic energy of the water jet per unit volume. Primarily influenced by density and velocity, it can reflect the variations of jet velocity attenuation and entrained air quality.

$$P = \frac{1}{2}\rho v^2. \tag{6}$$

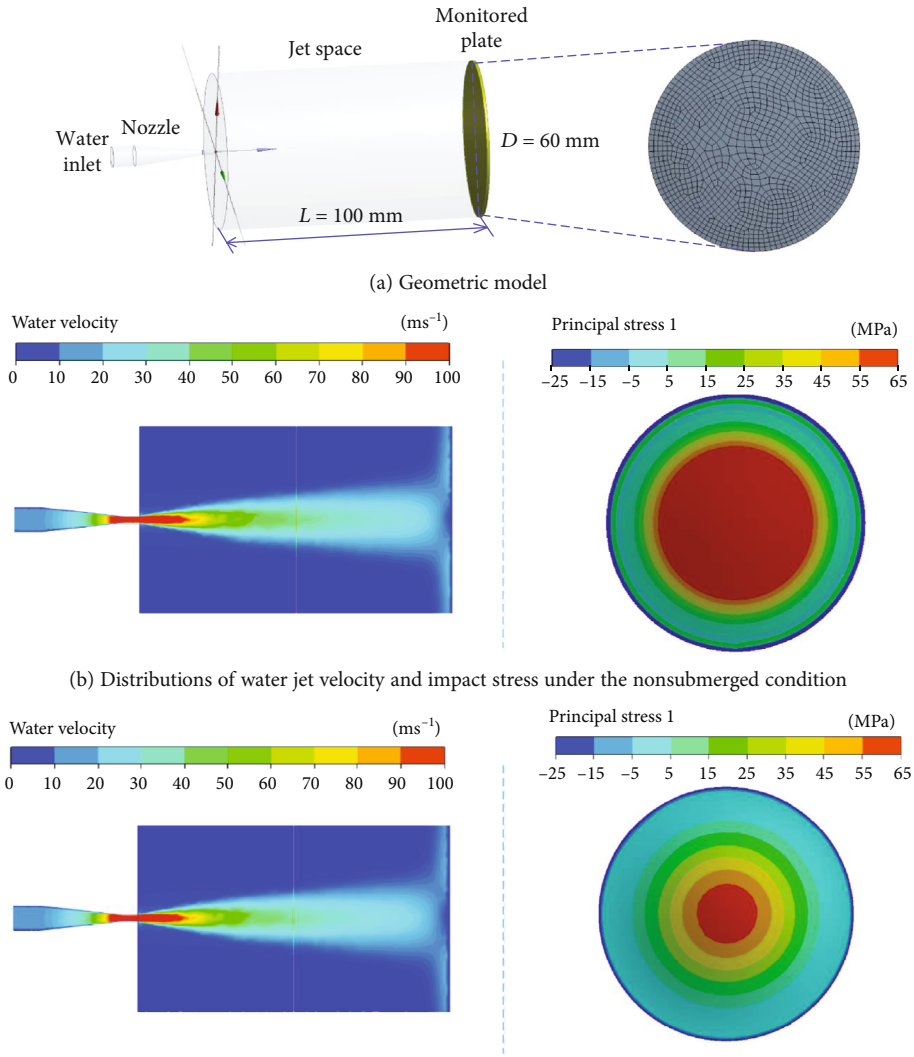

(a) Geometric model

(b) Distributions of water jet velocity and impact stress under the nonsubmerged condition

(c) Distributions of water jet velocity and impact stress under the submerged condition

Figure 4: Comparison between jet impact effects under the nonsubmerged and submerged conditions.

Under the nonsubmerged condition, the basic section is the major section that acts to crush the rock. The impact dynamic pressure distribution on each cross-section at different target distances in the initial section can be expressed as follows:

$$\frac{P}{P_m} = f(\eta) = \left(1 - \left(\frac{Y}{R}\right)^{1.5}\right)^2, \tag{7}$$

where P is the impact dynamic pressure, MPa; P_m is the dynamic pressure on the jet axis, MPa; R is the radius of the water jet cross-section, m; Y is the radial distance from the monitored point to the axis, m.

To investigate the impact dynamic pressure variations of HPWJ at different target distances (distances from the nozzle x) and different radial distances from the jet axis y, rigid plates were set at different target distances so that the problem was converted into HPWJ impact on the plate, as illustrated in Figure 5(a). The variations of maximum impact pressure on the monitored plate at different impact distances are presented in Figure 6. Among them, the contour maps of jet velocity and the distributions of maximum principal stress on the plate at the target distances of 10 mm, 30 mm, 70 mm, and 120 mm are shown in Figures 5(b)–5(e).

With the increase in the target distance, the jet velocity and the maximum impact pressure decrease gradually. The maximum impact pressure is as high as 188.1 MPa at the target distance of 10 mm, but it drops by 71.8% to 53.1 MPa at the target distance of 120 mm. The stress concentration zone at the cross-section center gradually expands with the increase in the target distance, which corresponds to the radial diffusion that occurs during jet impact. As the water jet keeps expanding forward, its cross-sectional area grows gradually. After being blocked by the plate, the water jet deflects to both sides. Gradually, the fluid on the jet axis expands and deflects to both sides for a longer distance. However, it fails to diffuse effectively in a short time and thus accumulates there. A fluid accumulation area with a lower jet velocity can be observed in the middle of the contact surface

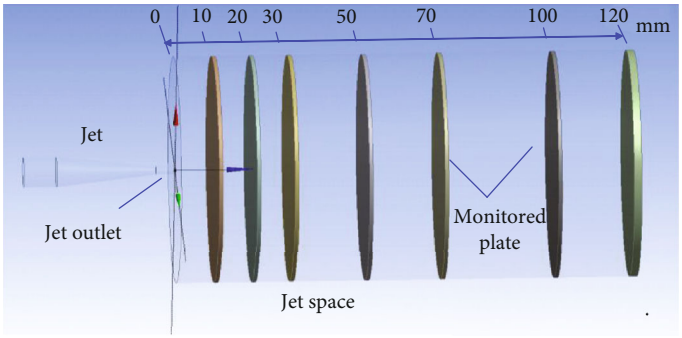

(a) Geometric model

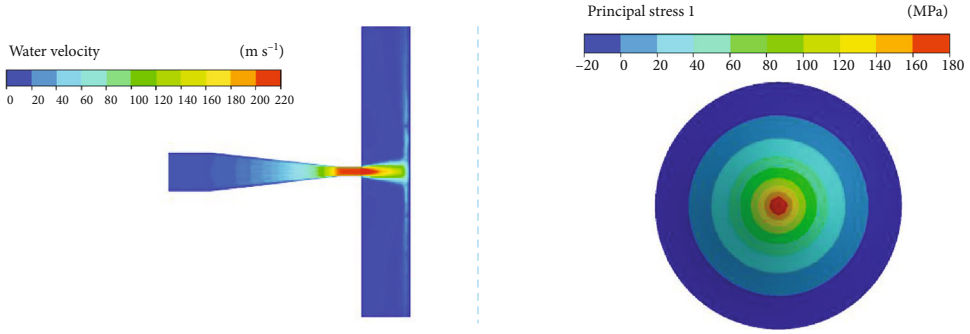

(b) Jet velocity and impact stress distribution on the plate at a target distance of 10 mm

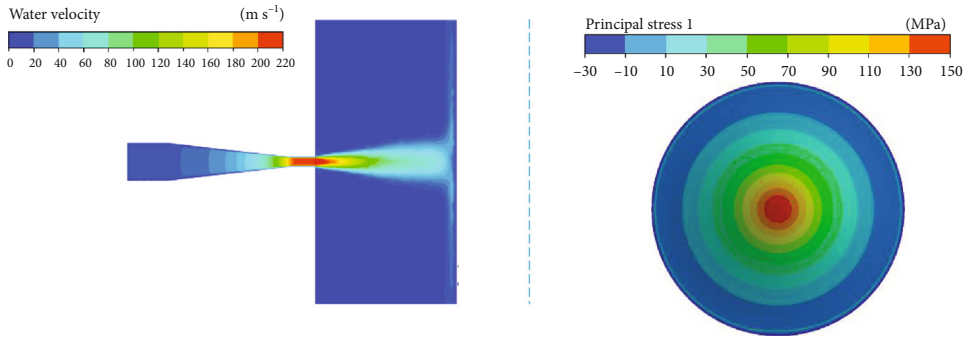

(c) Jet velocity and impact stress distribution on the plate at a target distance of 30 mm

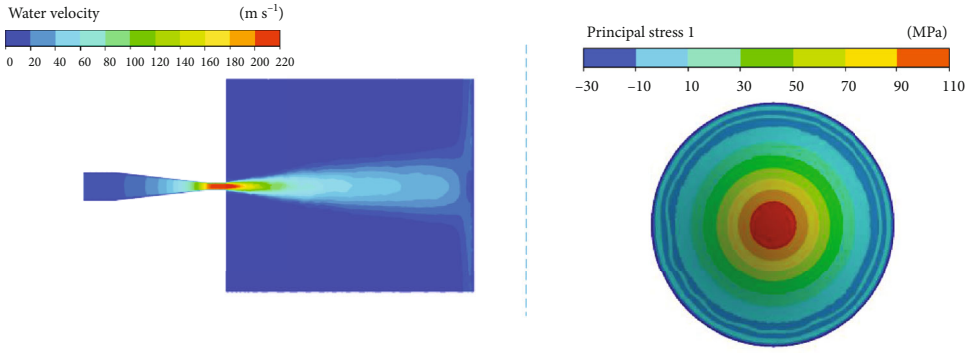

(d) Jet velocity and impact stress distribution on the plate at a target distance of 70 mm

Figure 5: Continued.

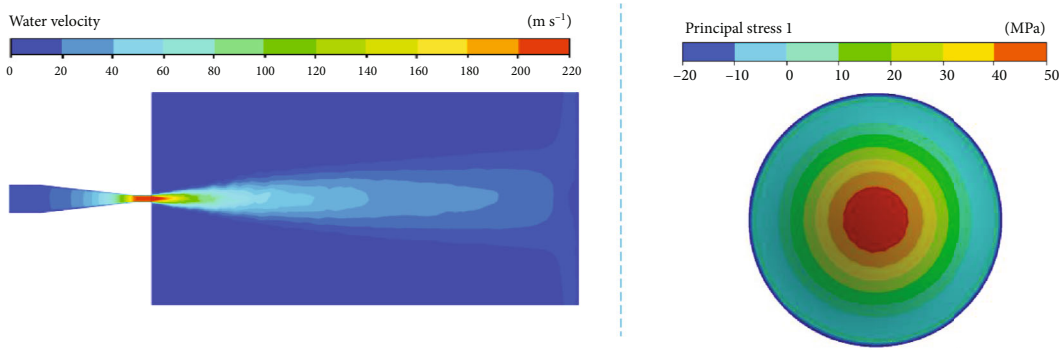

(e) Jet velocity and impact stress distribution on the plate at a target distance of 120 mm

Figure 5: Velocity and stress distribution of HPWJ impact on the plate at different target distances.

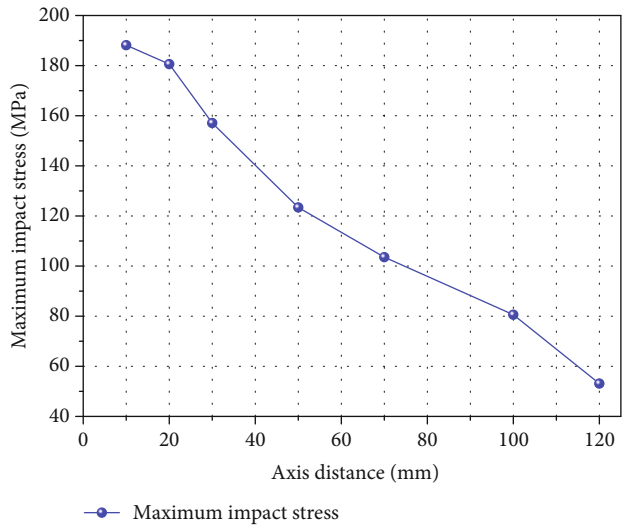

Figure 6: Impact pressure of HPWJ on the plate at different target distances.

between the jet and the plate in Figures 5(d) and 5(e). Despite the low jet velocity in this area, the transmission of fluid impact force is not affected.

3. Energy-Gathering Effect of the Conical-Cylindrical Combined Nozzle

3.1. Influence of the Nozzle Structure on the Jet Impact Effect. The nozzle, the executive element of the HPWJ generator, is responsible for converting energy. It gathers the pressure energy of the high-pressure water flow through the contraction of its internal cross-section, hence ensuring the excellent flow characteristics and dynamic performance of the water jet [62]. The nozzle structure has a crucial effect on jet properties such as the impact force, diffusion angle, and effective impact distance. The common nozzle structure and jet flow characteristics are illustrated in Figure 7.

The nozzle characteristic parameters affecting the jet impact performance mainly include the contraction angle α, length-diameter ratio l/d, contraction section length, and outlet diameter. With the aid of a high-speed camera, Lu et al. [63] captured the shape of water jet impact under different nozzle diameters and jet pressures. Besides, they made a statistical analysis on the jet diffusion angle and drew the following conclusions. First, when the water pressure is constant, the jet diffusion angle grows notably with the increase in the nozzle diameter. Second, when the nozzle diameter is constant, the diffusion angle changes slightly with the change in the water pressure. The second conclusion deviates from the conclusion given in Section 2.3 of this paper, probably due to limitations of the test equipment or the monitoring method.

Aiming at discussing the influence of the contraction angle on jet velocity attenuation, nonsubmerged water jet models whose contraction angles were 13°, 24°, 60°, 90°, and 180° were constructed, respectively. The water jet space in the model was a cylinder space with a diameter of 60 mm and a length of 200 mm. The inlet and outlet diameters of the nozzles were 4 mm and 1 mm, respectively. The contour maps of jet velocity formed by the nozzles are presented in Figure 8, and the jet velocity attenuation on the jet axis is shown in Figure 9. The contraction angle significantly influences the jet velocity. As the contraction angle grows, the jet velocity at the nozzle outlet falls and the jet attenuation rate rises. After the inlet and outlet diameters are determined, the total length of the nozzle is mainly determined by the contraction section length which is negatively correlated with the contraction angle. The nozzle adopted for hydraulic flushing in underground coal mines should not be too long, and the energy-gathering effect and the jet velocity attenuation amplitude are both acceptable under the contraction angle of 24°. Considering the two factors, 24° is the recommended contraction angle.

After being accelerated by the nozzle, the water jet is ejected in a cone shape. The jet velocity declines gradually in the axial direction, while it expands and diffuses gradually to both sides in the radial direction. When the nozzle contraction angle is set to 13°, the variations of jet velocity on the radial cross-sections at different axial distances are exhibited in Figure 10.

3.2. Influence of the Nozzle Angle on the Jet Shape. The nozzle, arranged on the side of the drill bit or drill pipe, forms a certain angle (denoted as α) with the drill pipe axis. The angle between the water jet and the normal of the coal wall

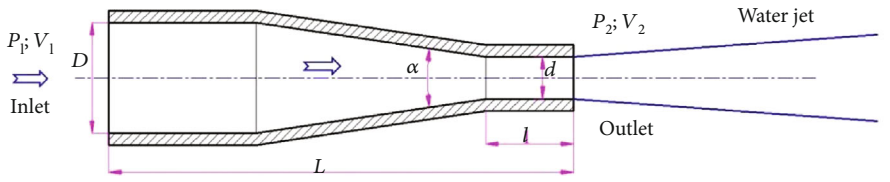

Figure 7: Nozzle structure and jet flow characteristics.

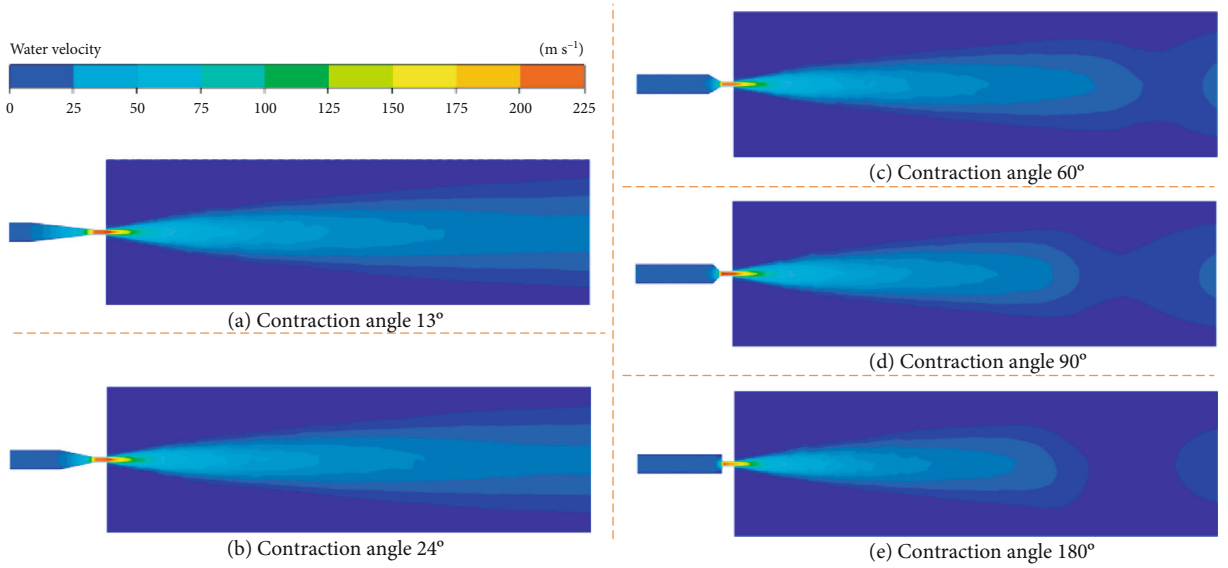

Figure 8: Contour maps of jet velocity formed by nozzles with different contraction angles.

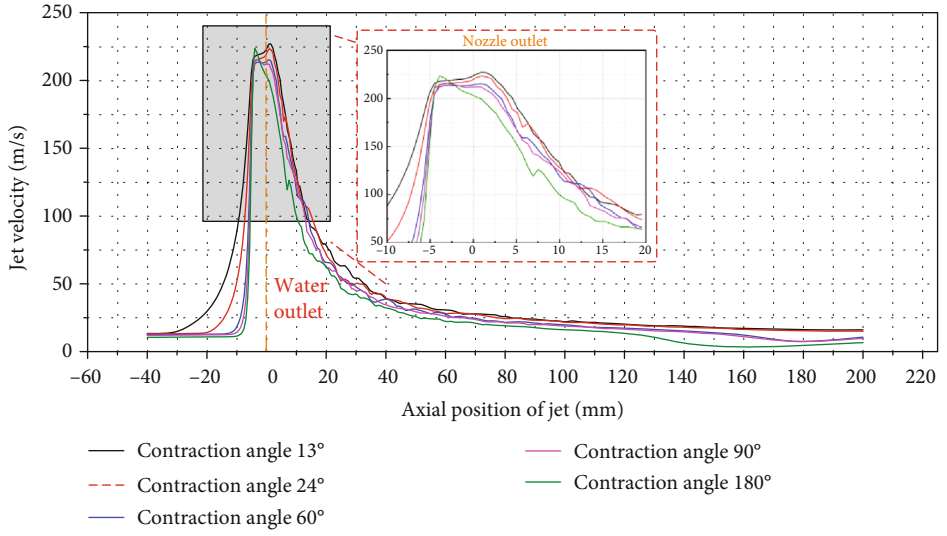

Figure 9: Variations of jet velocity on the jet axis under different contraction angles.

(denoted as β) whose value is determined by α shares a complementary angle with α. In this section, the influence of the nozzle angle on the jet shape and impact force is discussed in three cases, $\alpha = 90^\circ$, $\alpha = 60^\circ$, and $\alpha = 30^\circ$. The simulation results are shown in Figure 11. With the decrease in the nozzle angle, the turbulence degree of the fluid at the nozzle inlet decreases; the jet velocity increases; and the effective impact distance lengthens.

4. Influence of the Rotation Rate on the Impact Shape and Stress of HPWJ

4.1. Influence of Pump Pressure on HPWJ. The pressure of the high-pressure water pump station used for hydraulic flushing in underground coal mines generally lies within 10~60 MPa (10~40 MPa in most cases). In this study, the HPWJs generated at the pump pressures of 45 MPa, 35 MPa, 25 MPa, 15

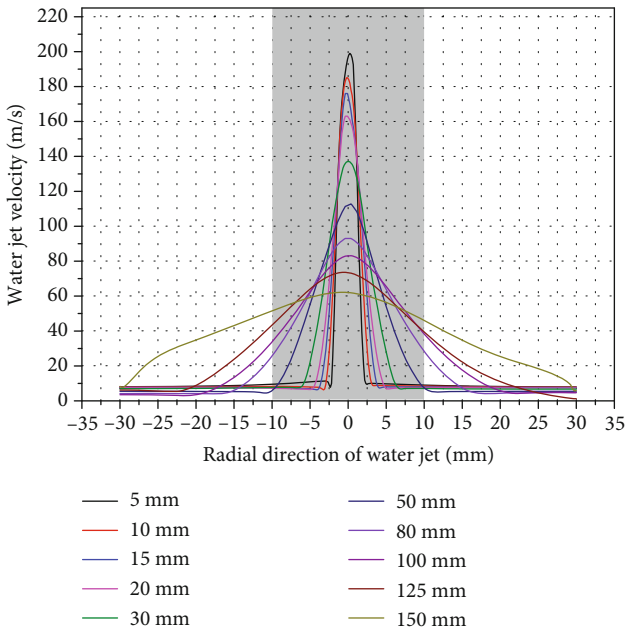

Figure 10: Variations of jet velocity on the radial cross-sections at different target distances.

MPa, and 10 MPa were numerically simulated. The simulation results are displayed in Figures 12 and 13.

The jet velocity on the jet axis rises gradually with the increase in the pump pressure, so does the acceleration of the jet when it passes through the nozzle. The maximum jet velocity at the nozzle outlet is as high as 305 m/s at the pump pressure of 45 MPa, while it drops to 143 m/s when the pump pressure is reduced to 10 MPa. On the other hand, an excessive pump pressure will result in an increase in the jet diffusion angle and a strong interaction between the jet and the air. The large amount of entrained air promotes the breakage and separation of water. As a result, the atomization of water intensifies. In the case of constant sizes of the jet pipe and nozzle, when the pump pressure remains low, the effective impact distance (compact section and core section) of the jet lengthens with the increase in it; when the pump pressure increases to a certain extent, raising it further will lead to the atomization of water; that is, water breaks into small droplets under the action of air. Under a higher pump pressure, the atomization of water is more intensified, and thus, the effective impact distance is shorter. For underground hydraulic flushing operation equipment in coal mines, there exists an optimal range of pump pressure where the jet can reach the best effective impact distance and impact force. Moreover, since the distance between the nozzle and the coal wall gradually expands as the flushing proceeds, the pump pressure needs to be constantly adjusted to keep the coal wall within the effective impact distance. When the distance between the nozzle and the coal wall reaches a certain limit, raising the pump pressure further will strengthen the atomization of water, failing to prolong the effective impact distance of the jet. Hence, an upper limit exists for the depth of coal crushing by the same equipment.

4.2. Different Stages of Coal Crushing by HPWJ. According to the shape of the coal pit formed by HPWJ impact, the process of coal crushing can be roughly divided into three stages, namely, the concave stage, the conical pit stage, and the cylindrical pit stage. In the initial stage of coal crushing, the jet rushes to the coal wall almost vertically after being accelerated by the nozzle, as shown in Figure 14(a). The coal at the jet axis, which undergoes the largest impact force, starts to break and fall off first, and a conical pit with a certain angle appears on the coal wall there, as presented in Figure 14(b). As the coal keeps breaking and falling off, the pit deepens and becomes cylindrical, as exhibited in Figure 14(c). The difference in the coal wall shape exerts an enormous effect on the distribution of jet velocity. Blocked by the coal wall, the jet changes its direction to varying degrees. In this process, part of the momentum in the original jet direction will be lost and transferred to the coal in the form of force. On the other hand, the jet velocity gradually attenuates with the increase in the target distance, and the increase in the pit depth will induce water accumulation at the bottom of the pit. In this study, the coal wall formed by HPWJ impact was appropriately simplified into a regular smooth slope, and the influence of crushed coal slag on the jet was ignored. Under this assumption, a numerical model was built to investigate the influence of different coal wall shapes on the jet impact effect (Figure 15).

As the impacted coal breaks and separates gradually, the jet experiences the plane impact stage, the conical impact stage, and the cylindrical impact stage in turn. Blocked by the coal wall, water at the bottom of the pit is discharged at a decelerated rate and accumulates there, forming a cushion on the coal wall surface. Consequently, the nonsubmerged jet is progressively converted to a submerged jet at the bottom of the pit. The HPWJ can hardly directly act on the coal surface so that the jet impact force is greatly reduced. In addition, due to the increase in the pit depth, the broken coal slag on the coal wall has to cross a longer distance to be discharged. Meanwhile, the decelerated discharge of the jet from the pit will weaken its slag removal ability. The crushed coal slag that cannot be discharged in time also buffers the coal wall from the jet impact. Under the comprehensive effect of the above factors, the HPWJ finds it difficult to crush the coal in a deeper area.

4.3. Influence of the Rotation Rate on the Jet Shape. During borehole construction in soft broken coal, the borehole collapses and gets blocked easily. To ensure the successful construction of boreholes, drilling is often conducted at a high rotation speed using a large-blade spiral drill pipe so that the coal slag can be discharged smoothly. In the hydraulic flushing process, the drill pipe also needs to rotate at a certain speed, which is not only required by the nozzle for rotary coal crushing but also conducive to the discharge of coal slag. The influence of rotation on the jet in the rotary flushing process is exhibited in Figure 16. When the jet leaves the nozzle to impact the coal wall, it deflects as a result of inertia, and the jet axis is no longer straight. The jet becomes less continuous, and the rear jet has a weaker effect on the front jet. Resultantly, the jet impact force becomes too

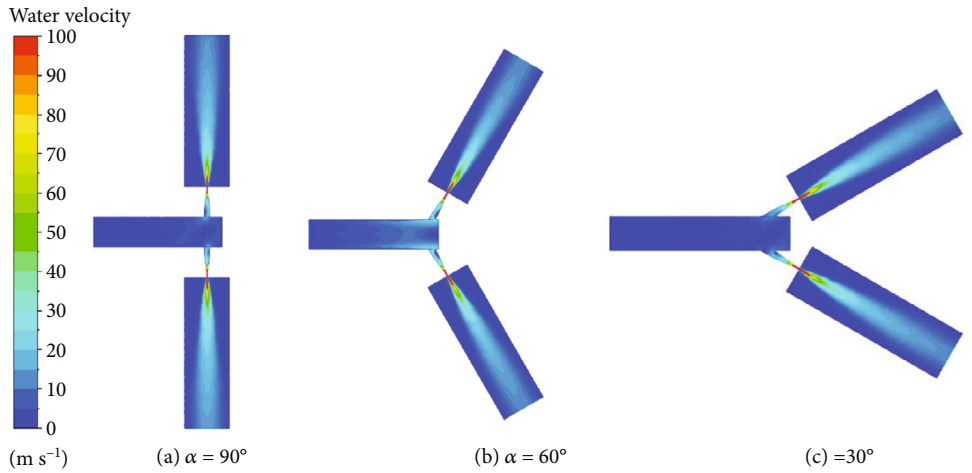

Figure 11: Contour maps of jet velocities under different nozzle angles.

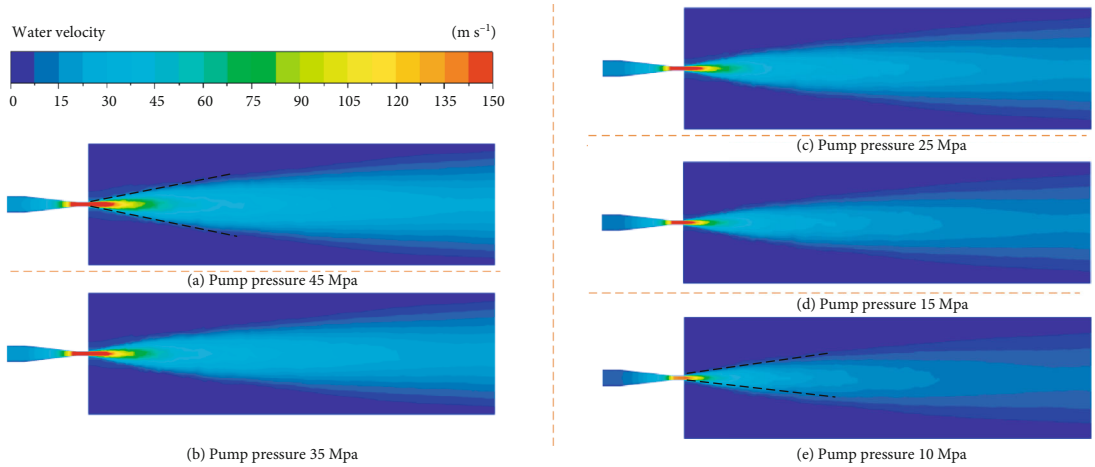

Figure 12: HPWJs generated at different pump pressures.

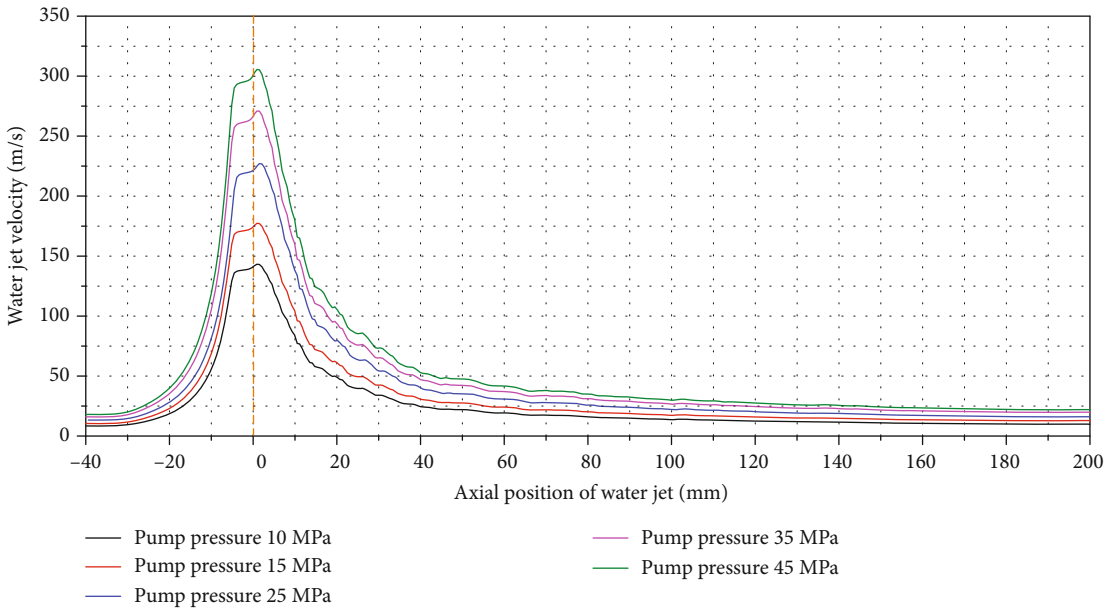

Figure 13: Variations of jet velocity on the jet axis at different pump pressures.

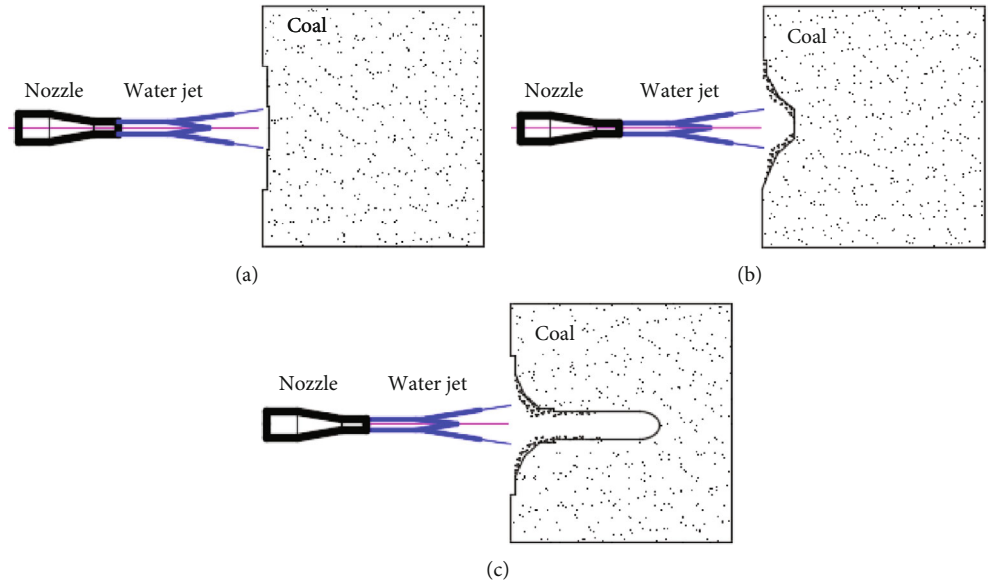

Figure 14: Different stages of HPWJ-induced coal crushing.

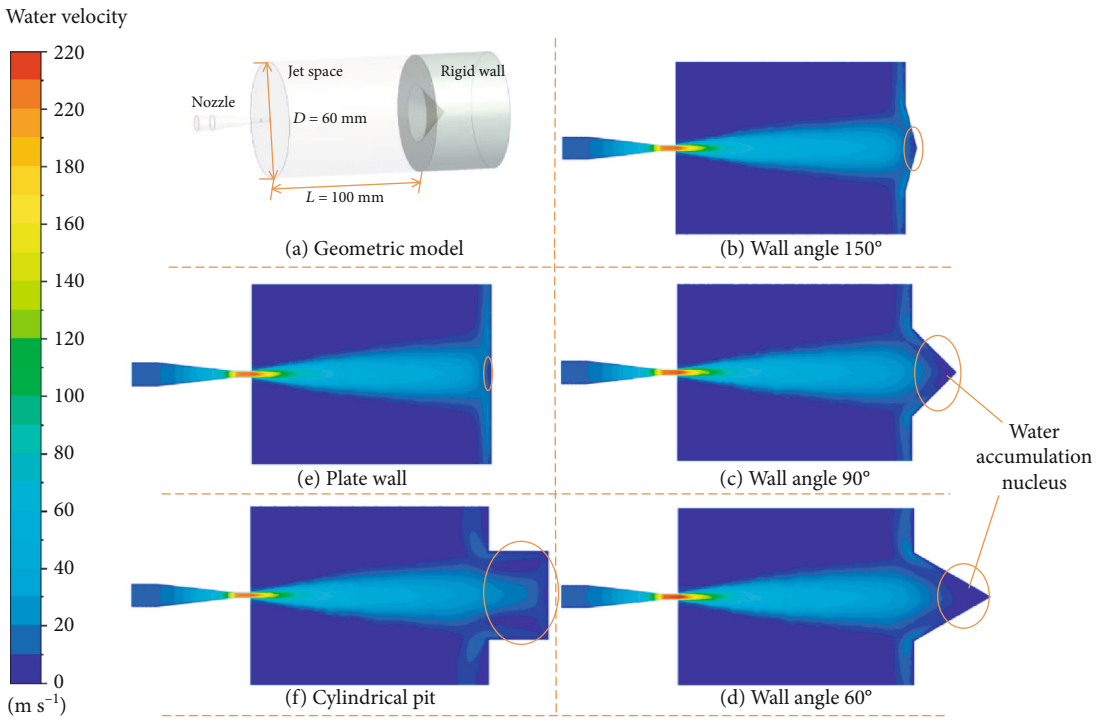

Figure 15: Contour maps of jet velocity in different coal crushing stages.

weak to guarantee the impact distance. The rotation speeds commonly used in drilling and hydraulic operations in coal mines lie in the range of 30-300 r/min. In this study, the jet shapes in this range were comparatively analyzed. The simulation results for the two-nozzle combination and the three-nozzle combination are given in Figures 17 and 18, respectively.

Under both combination modes, the jet shapes exhibit resembling variation trends with the rotation speed. For the two-nozzle combination, when the rotation speed is as high as 300 r/min, the jet deviates sharply for approximately 90° after leaving from the nozzle, with the maximum impact distance being about 20 mm. When the rotation speed is reduced to 180 r/min, the jet deviates less violently, with the maximum impact distance being about 80 mm. As the rotation speed decreases to 120 r/min, the jet deviation angle continues to narrow while the impact distance lengthens. As the rotation speed decreases to 90 r/min, the jet gradually

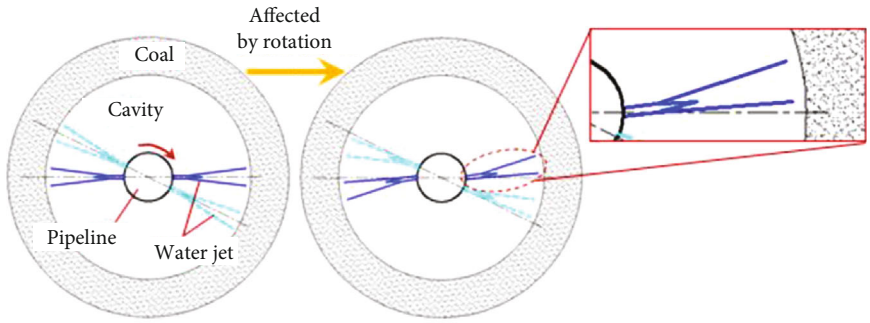

Figure 16: Influence of the rotation speed on the shape of HPWJ.

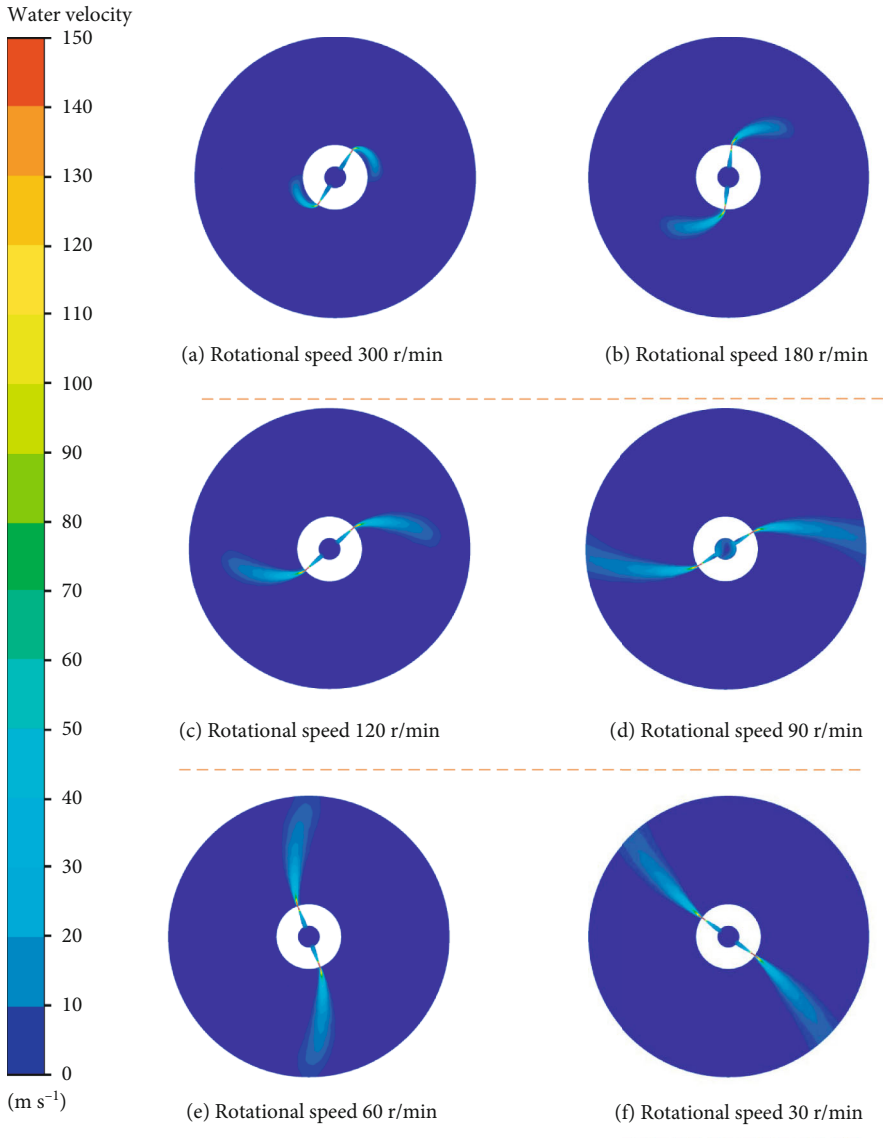

Figure 17: Contour maps of jet velocity for the two-nozzle combination at different rotation speeds.

reaches the boundary (200 mm) of the model. Compared with the front end of the jet, the initial section has a smaller deviation angle. As the rotation speed drops to 30 r/min, the jet only has a small deflection angle.

In summary, the nozzle rotation speed remarkably influences the jet shape and the impact distance. Rotation of the nozzle will lead to the deflection of the jet. The deflection angle grows with the increase in the rotation speed. It can

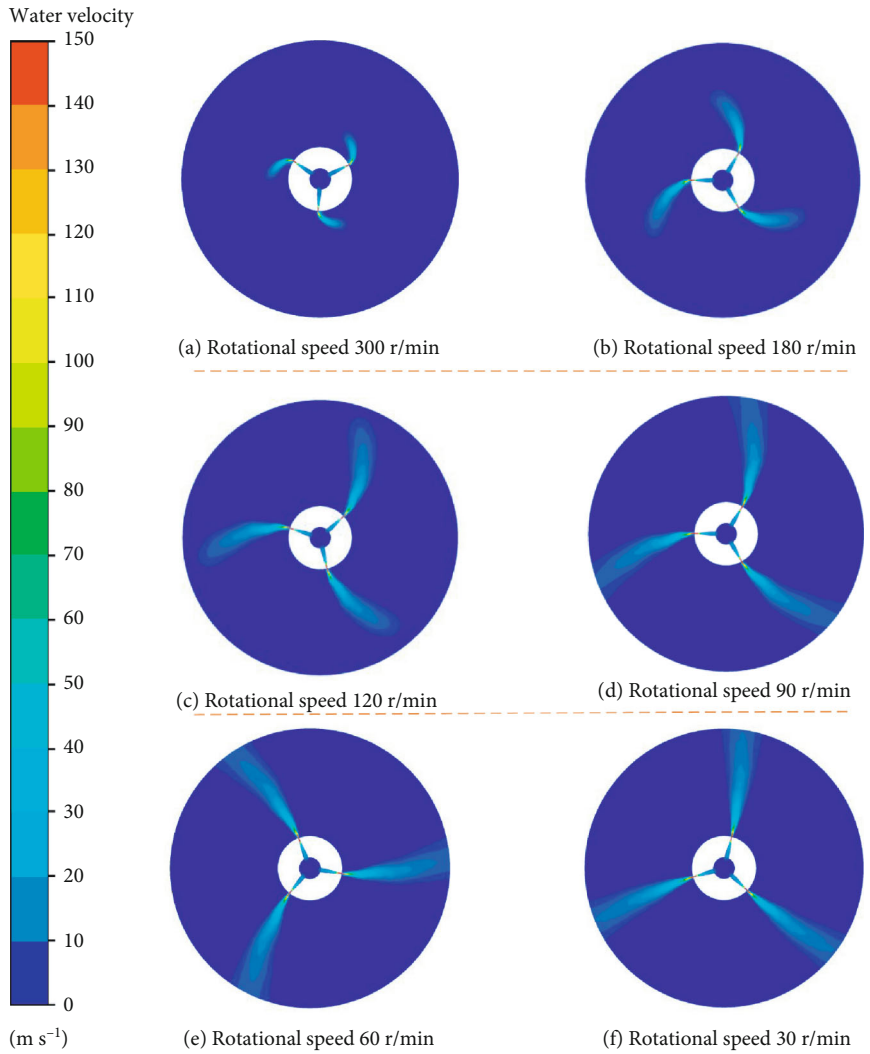

Figure 18: Contour maps of jet velocity for the three-nozzle combination at different speeds.

be as high as 90° when the rotation speed is high enough. Besides, the influence of the rotation speed on the deflection angle is more significant at a longer impact distance. The deflection of the jet worsens the jet continuity, shortens the impact distance, and weakens the impact force. When the rotation speed is low, only the fracture section and the dissipation section are affected. As the rotation rate rises, the initial section is also affected. An excessively high rotation speed will shorten the effective impact distance, reduce the coal crushing depth, and lower the coal crushing efficiency. On the other hand, as can be known from the analysis in the previous section, an upper limit exists for the depth of coal crushing by the same equipment under a constant pump pressure. When this upper limit is reached, the pit no longer changes with the passage of flushing time. If the nozzle rotation speed is too low, the flushing will be time-consuming and unable to achieve an improved flushing effect, which will not only delay the construction period but also waste water resources. Moreover, after the jet sweeps over the coal surface, the reflection of compression waves generated in the coal also contributes to coal crushing. An excessively low rotation speed will weaken the reflection and coal crushing performance of compression waves.

5. Conclusions

In this paper, the axial and radial stress distributions of the high-pressure water jet (HPWJ) and the energy-gathering effect of a conical-cylindrical combined nozzle were analyzed by simulation. Furthermore, the influences of the submergence conditions, nozzle angle, pump station pressure, rotation speed on the shape, and impact pressure of HPWJ were explored. The main conclusions are as follows:

(1) In the radial direction, the submerged condition will accelerate the attenuation of jet velocity and reduce the impact strength of the jet. The jet impact force on the axis of the rigid plate with the target distance of 100 mm can reach 80.7 MPa under the nonsubmerged condition, while it drops to 65.2 MPa by 19.2% under the submerged condition. In the axial direction, the jet velocity and the impact force both

decline gradually with the increase in the target distance under the nonsubmerged condition. The maximum impact pressure is as high as 188.1 MPa at the target distance of 10 mm, but it weakens to 53.1 MPa by 71.8% at the target distance of 120 mm

(2) After the nozzle inlet and outlet diameters are determined, the total length of the nozzle is mainly determined by the contraction angle. Considering that the nozzle adopted for hydraulic flushing in underground coal mines should not be too long, 24° is the recommended contraction angle

(3) During coal wall crushing by HPWJ, blocked by the coal wall, water at the bottom of the pit is discharged at a decelerated rate and accumulates there. Consequently, the nonsubmerged jet is gradually converted to the submerged jet at the bottom of the pit. In addition, the rotation speed should be controlled within 90 r/min in order to increase the coal crushing efficiency

Data Availability

The data used to support the results of this study are available from the corresponding author upon request.

Conflicts of Interest

The authors declare that they have no conflicts of interest.

Acknowledgments

This research was financially supported by the Shanghai Rising-Star Program (20QB1401000), National Science Foundation of China (51804176, 51706122), Natural Science Foundation of Shanghai (19ZR1411500), Natural Science Foundation of Shandong Province (ZR2018PEE001), Science & Technology Foundation of Guizhou Province ([2020]4Y055), China Postdoctoral Science Foundation (2019M652346), and Project of Shandong Province Higher Educational Science and Technology Program (J18KA187).

References

[1] J. Liu, R. Zhang, D. Z. Song, and Z. Q. Wang, "Experimental investigation on occurrence of gassy coal extrusion in coalmine," *Safety Science*, vol. 113, pp. 362–371, 2019.

[2] S. Q. Lu, Y. L. Zhang, Z. Y. Sa, S. F. Si, L. Y. Shu, and L. Wang, "Damage-induced permeability model of coal and its application to gas predrainage in combination of soft coal and hard coal," *Energy Science & Engineering*, vol. 7, no. 4, pp. 1352–1367, 2019.

[3] Q. Ma, W. Nie, S. Yang et al., "Effect of spraying on coal dust diffusion in a coal mine based on a numerical simulation," *Environmental Pollution*, vol. 264, p. 114717, 2020.

[4] Z. Xiu, W. Nie, J. Yan et al., "Numerical simulation study on dust pollution characteristics and optimal dust control air flow rates during coal mine production," *Journal of Cleaner Production*, vol. 248, p. 119197, 2020.

[5] Y. Hua, W. Nie, Q. Liu, H. Peng, W. Wei, and P. Cai, "The development and application of a novel multi-radial-vortex-based ventilation system for dust removal in a fully mechanized tunnelling face," *Tunnelling and Underground Space Technology*, vol. 98, p. 103253, 2020.

[6] W. Niu, W. Nie, M. Yuan et al., "Study of the microscopic mechanism of lauryl glucoside wetting coal dust: environmental pollution prevention and control," *Journal of Hazardous Materials*, vol. 412, p. 125223, 2021.

[7] H. Wang, Z. Y. Sa, W. M. Cheng, R. Zhang, and S. Yang, "Effects of forced-air volume and suction region on the migration and dust suppression of air curtain during fully mechanized tunneling process," *Process Safety and Environmental Protection*, vol. 145, pp. 222–235, 2021.

[8] H. Xu, S. Sang, J. Yang, and H. Liu, "CO2 storage capacity of anthracite coal in deep burial depth conditions and its potential uncertainty analysis: a case study of the No. 3 coal seam in the Zhengzhuang Block in Qinshui Basin, China," *Geosciences Journal*, 2021.

[9] J. Liu, "Technic study on increasing permeability of deep-hole presplitting blasting and its application in low permeability coal seam," AnHui University of Science and Technology, Ph.D., 2008.

[10] W. L. Quan, J. M. Xv, S. H. Tu, D. S. Zhang, and X. Q. Liang, *Introduction to Mining Engineering*, China University of Mining and Technology Press, Xuzhou, 2004.

[11] F. Du and K. Wang, "Unstable failure of gas-bearing coal-rock combination bodies: insights from physical experiments and numerical simulations," *Process Safety and Environmental Protection*, vol. 129, pp. 264–279, 2019.

[12] S. Lu, C. Wang, M. Li et al., "Gas time-dependent diffusion in pores of deformed coal particles: model development and analysis," *Fuel*, vol. 295, p. 120566, 2021.

[13] Q. Bao, W. Nie, C. Liu et al., "The preparation of a novel hydrogel based on crosslinked polymers for suppressing coal dusts," *Journal of Cleaner Production*, vol. 249, pp. 119–343, 2020.

[14] F. Chen, A. Cao, L. Dou, and G. Jing, "A quantitative evaluation method of coal burst hazard based on zone division and an analytic hierarchy process: a case study on Yanbei coal mine, Gansu Province, China," *Geosciences Journal*, vol. 23, no. 5, pp. 833–848, 2019.

[15] S. Lu, C. F. Wang, Q. Q. Liu et al., "Numerical assessment of the energy instability of gas outburst of deformed and normal coal combinations during mining," *Process Safety and Environmental Protection*, vol. 132, pp. 351–366, 2019.

[16] F. Du, K. Wang, X. Zhang, C. P. Xin, L. Y. Shu, and G. D. Wang, "Experimental study of coal-gas outburst: insights from coal-rock structure, gas pressure and adsorptivity," *Natural Resources Research*, vol. 29, no. 4, pp. 2481–2493, 2020.

[17] X. Liu, W. Nie, Y. Hua, C. Liu, L. Guo, and W. Ma, "Behavior of diesel particulate matter transport from subsidiary transportation vehicle in mine," *Environmental Pollution*, vol. 270, p. 116264, 2021.

[18] M. Y. Chen, Y. P. Cheng, J. C. Wang, H. R. Li, and N. Wang, "Experimental investigation on the mechanical characteristics of gas-bearing coal considering the impact of moisture," *Arabian Journal of Geosciences*, vol. 12, no. 18, 2019.

[19] S. Q. Lu, L. Li, Y. Q. Cheng, Z. Y. Sa, Y. L. Zhang, and N. Yang, "Mechanical failure mechanisms and forms of normal and deformed coal combination containing gas: model development and analysis," *Engineering Failure Analysis*, vol. 80, pp. 241–252, 2017.

[20] R. Zhang, J. Liu, Z. Y. Sa, Z. Q. Wang, S. Q. Lu, and C. F. Wang, "Experimental investigation on multi-fractal characteristics of acoustic emission of coal samples subjected to true triaxial loading-unloading," *Fractals-Complex Geometry Patterns and Scaling in Nature and Society*, vol. 28, 2020.

[21] Y. Han, B. W. Dong, F. Y. Zhang, S. Lv, and W. D. Li, "Process of hydraulic punching technology for relieving pressure and enhancing permeability in China," *China Mining Magazine*, vol. 30, pp. 95–100, 2021.

[22] H. M. Yang, X. L. Qiu, and X. L. Lv, "Numerical simulation of effective influence radius of hydraulic cavitation model of "one hole and multiple cavitation"," *Coal Technology*, vol. 40, 2021.

[23] H. L. Liao, G. S. Li, and J. L. Niu, "Influential factors and mechanism analysis of rock breakage by ultra-high pressure water jet under submerged condition," *Chinese Journal of Rock Mechanics and Engineering*, vol. 27, pp. 1243–1250, 2008.

[24] Y. Y. Lu, X. H. Li, and W. Y. Xiang, "Rock erosion mechanism of cavitating water jets," *Rock and Soil Mechanics*, vol. 26, pp. 1233–1237, 2005.

[25] F. B. Tian and M. Lin, "Studies on the mechanism of water jet - assisted drilling technology(1)——cavitation and erosion," *Mechanics in Engineering*, vol. 29, pp. 29–33, 2007.

[26] F. B. Tian and M. Lin, "Studies on the mechanism of water jet - assisted drilling technology(2)—— high-speed drip impacting with solid target," *Mechanics in Engineering*, vol. 29, pp. 34–39, 2007.

[27] M. M. Singh and H. L. Hartman, "Hypothesis for the mechanism of rock failure under impact," *The 4th U.S. Symposium on Rock Mechanics (USRMS) University Park*, 1961American Rock Mechanics Association, Pennsylvania, 1961.

[28] I. W. Farmer and P. B. Attewell, "Rock penetration by high velocity water jet: a review of the general problem and an experimental study," *International Journal of Rock Mechanics and Mining Sciences & Geomechanics Abstracts*, vol. 2, no. 2, pp. 135–153, 1965.

[29] C. Pan and Y. Yao, "The numerical simulation of rock fragmentation by high-pressure jet," *China Rural Water and Hydropower*, vol. 12, pp. 59–62, 2005.

[30] Z. H. Bai and L. W. Cao, "Numerical simulation and analysis of rock breaking under pulse water jet," *Journal of Chongqing University of Technology(Natural Science)*, vol. 23, pp. 31–35, 2009.

[31] L. Ma, R. Bao, and Y. M. Guo, "Waterjet penetration simulation by hybrid code of SPH and FEA," *International Journal of Impact Engineering*, vol. 35, 2007.

[32] J. Wang, N. Gao, and W. Gong, "Abrasive waterjet machining simulation by coupling smoothed particle hydrodynamics/finite element method," *Chinese Journal of Mechanical Engineering*, vol. 23, no. 5, pp. 568–573, 2010.

[33] K. Maniadaki, T. Kestis, N. Bilalis, and A. Antoniadis, "A finite element-based model for pure waterjet process simulation," *The International Journal of Advanced Manufacturing Technology*, vol. 31, no. 9-10, pp. 933–940, 2007.

[34] W. J. Gong, J. M. Wang, and N. Gao, "Numerical simulation for abrasive water jet machining based on ALE algorithm," *The International Journal of Advanced Manufacturing Technology*, vol. 53, no. 1-4, pp. 247–253, 2011.

[35] H. J. Ni and R. H. Wang, "A theoretical study of rock drilling with a high pressure water jet," *Petroleum Science*, vol. 1, no. 4, pp. 72–76, 2004.

[36] H. J. Ni, R. H. Wang, and Y. H. Bai, "Finite element method for analyzing high-pressure water jet breaking rock," *Journal of China University of Petroleum(Edition of Natural Science)*, vol. 37, p. 40, 2002.

[37] H. J. Ni, R. H. Wang, and H. K. Ge, "Numerical simulation on rock breaking under high pressure water," *Chinese Journal of Rock Mechanics and Engineering*, vol. 23, pp. 550–554, 2004.

[38] H. J. Ni, R. H. Wang, and Y. Q. Zhang, "Numerical simulation study on rock breaking mechanism and process under high pressure water jet," *Applied Mathematics and Mechanics*, vol. 26, no. 12, pp. 1445–1452, 2005.

[39] R. H. Wang and H. J. Ni, "Research of rock fragmentation mechanism with high-pressure water jet," *Journal of China University of Petroleum(Edition of Natural Science)*, vol. 26, pp. 118–122, 2002.

[40] R. H. Wang, Z. H. Shen, and W. D. Zhou, "Experimental study on rock breaking borehole by high pressure water jet," *Oil Drilling & Production Technology*, vol. 20-25, pp. 99-100, 1995.

[41] Z. C. Song and J. M. Chen, "Numerical simulation for high-pressure water jet breaking rock mechanism based on SPH algorithm," *Oil Field Equipment*, vol. 38, pp. 39–43, 2009.

[42] Y. Y. Lu, S. Zhang, Y. Liu, Z. H. Lu, and L. Y. Jiang, "Analysis on stress wave effect during the process of rock breaking by pulsed jet," *Journal of Chongqing University*, vol. 35, pp. 117–124, 2012.

[43] J. L. Liu and H. Si, "Numerical simulation on damage field of high pressure water jet breaking rock under high ambient pressure," *Journal of Chongqing University*, vol. 34, pp. 40–46, 2011.

[44] H. Si, Y. M. Xie, and C. H. Yang, "Numerical simulation of rock damage field under abrasive water jet," *Rock and Soil Mechanics*, vol. 32, pp. 935–940, 2011.

[45] Q. Li, "Research on driling long hole in soft coal seam by high pressure water jets," Chongqing University, 2008.

[46] W. Z. Jiang, "Research on theory of slotting and enhancing permeability by high pressure rotational jetting in low permeability coal seam and its application," China University of Mining and Technology, 2009.

[47] X. Zhang, "The study on the mechanism and experiment of high pressure water jet slotted," Liaoning Technical University, 2009.

[48] X. C. Wang, Y. Y. Lu, Y. Kang, B. W. Xia, and S. Zhang, "Experimental study of abrasive waterjet cutting coal-rock mass," *Journal of China University of Mining & Technology*, vol. 40, pp. 246–251, 2011.

[49] Q. D. Sun, Z. M. Wang, J. Q. Yu, and W. H. Zhang, "A disquisition on breaking mechanism of high pressure jet impacting on rock," *Rock and Soil Mechanics*, vol. 26, pp. 978–982, 2005.

[50] X. D. Lin, Y. Y. Lu, J. R. Tang, X. Ao, and L. Zhang, "Numerical simulation of abrasive water jet breaking rock with SPH-FEM coupling algorithm," *Journal of Vibration and Shock*, vol. 33, pp. 170–176, 2014.

[51] D. Sevda, "Experimental and numerical study of rock breakage by pulsed water jets," Australia University of Queensland, PhD, Brisbane, 2011.

[52] F. J. Heymann, "High-speed impact between a liquid drop and a solid surface," *Journal of Applied Physics*, vol. 40, no. 13, pp. 5113–5122, 1969.

[53] S. S. Cook, "Erosion by water-hammer," *Proceedings of the Royal Society of London Series A, Containing Papers of a*

Mathematical and Physical Character, vol. 119, no. 783, pp. 481–488, 1928.

[54] J. E. Field, "Stress waves, deformation and fracture caused by liquid impact," *Philosophical Transactions of the Royal Society of London Series A, Mathematical and Physical Sciences*, vol. 260, pp. 86–93, 1966.

[55] J. E. Field, "ELSI conference: invited lecture: liquid impact: theory, experiment, applications," *Wear*, vol. 233-235, pp. 1–12, 1999.

[56] K. Pianthong, S. Zakrzewski, M. Behnia, and B. E. Milton, "Supersonic liquid jets: their generation and shock wave characteristics," *Shock Waves*, vol. 11, no. 6, pp. 457–466, 2002.

[57] W. K. Soh, B. C. Khoo, and W. Y. D. Yuen, "The entrainment of air by water jet impinging on a free surface," *Experiments in Fluids*, vol. 39, no. 3, pp. 498–506, 2005.

[58] X. Q. Ma, *Impact Dynamics*, Beijing Institute of Technology Press, Beijing, 1992.

[59] R. H. Wang and H. J. Ni, "Study on rock breaking mechanism of high pressure water jet," China University of Petroleum Press, 2010.

[60] F. Huang, "On the transient dynamics of water jet impinging target and the mechanism of water jet breaking rock," Chongqing University, 2015.

[61] A. Ohashi and K. Yanaida, "The fluid mechanics of capsule pipelines : 1st report, analysis of the required pressure drop for hydraulic and pneumatic capsules," *JSME International Journal Series B-fluids and Thermal Engineering*, vol. 29, no. 252, pp. 1719–1725, 1986.

[62] Y. S. Yang, J. P. Zhang, and S. L. Nie, "Energy loss of nozzles in water jet system," *Journal of Mechanical Engineering*, vol. 49, no. 2, pp. 139–145, 2013.

[63] T. K. Lu, H. Yu, and Y. Dai, "Longhole waterjet rotary cutting for in-seam cross panel methane drainage," *Mining Science and Technology*, vol. 20, pp. 378–383, 2010.